(12) INTERNATIONAL APPLICATION PUBLISHED UNDER THE PATENT COOPERATION TREATY (PCT)

(19) World Intellectual Property Organization
International Bureau

(43) International Publication Date
29 November 2012 (29.11.2012)

WIPO | PCT

(10) International Publication Number
WO 2012/162391 A2

(51) **International Patent Classification**:
G01D 21/00 (2006.01) ***G01V 9/00*** (2006.01)
G01D 3/00 (2006.01)

(21) **International Application Number**:
PCT/US2012/039138

(22) **International Filing Date**:
23 May 2012 (23.05.2012)

(25) **Filing Language**: English

(26) **Publication Language**: English

(30) **Priority Data**:
61/489,855 25 May 2011 (25.05.2011) US

(71) **Applicant** *(for all designated States except US)*: **UNIVERSITY OF CENTRAL FLORIDA RESEARCH FOUNDATION, INC.** [US/US]; 12201 Research Parkway, Suite 501, Orlando, FL 32826 (US).

(72) **Inventor; and**
(75) **Inventor/Applicant** *(for US only)*: **YUN, Hae-Bum** [KR/US]; 331 Grey Owl Run, Chuluota, FL 32766 (US).

(74) **Agent**: **RISLEY, David, R.**; Thomas, Kayden, Horstemeyer & Risley, LLP., 400 Interstate North Parkway, Suite 1500, Atlanta, GA 30339 (US).

(81) **Designated States** *(unless otherwise indicated, for every kind of national protection available)*: AE, AG, AL, AM, AO, AT, AU, AZ, BA, BB, BG, BH, BR, BW, BY, BZ, CA, CH, CL, CN, CO, CR, CU, CZ, DE, DK, DM, DO, DZ, EC, EE, EG, ES, FI, GB, GD, GE, GH, GM, GT, HN, HR, HU, ID, IL, IN, IS, JP, KE, KG, KM, KN, KP, KR, KZ, LA, LC, LK, LR, LS, LT, LU, LY, MA, MD, ME, MG, MK, MN, MW, MX, MY, MZ, NA, NG, NI, NO, NZ, OM, PE, PG, PH, PL, PT, QA, RO, RS, RU, RW, SC, SD, SE, SG, SK, SL, SM, ST, SV, SY, TH, TJ, TM, TN, TR, TT, TZ, UA, UG, US, UZ, VC, VN, ZA, ZM, ZW.

(84) **Designated States** *(unless otherwise indicated, for every kind of regional protection available)*: ARIPO (BW, GH, GM, KE, LR, LS, MW, MZ, NA, RW, SD, SL, SZ, TZ, UG, ZM, ZW), Eurasian (AM, AZ, BY, KG, KZ, RU, TJ, TM), European (AL, AT, BE, BG, CH, CY, CZ, DE, DK, EE, ES, FI, FR, GB, GR, HR, HU, IE, IS, IT, LT, LU, LV, MC, MK, MT, NL, NO, PL, PT, RO, RS, SE, SI, SK, SM, TR), OAPI (BF, BJ, CF, CG, CI, CM, GA, GN, GQ, GW, ML, MR, NE, SN, TD, TG).

Published:

— *without international search report and to be republished upon receipt of that report (Rule 48.2(g))*

WO 2012/162391 A2

(54) **Title**: SYSTEMS AND METHODS FOR DETECTING SMALL PATTERN CHANGES IN SENSED DATA

(57) **Abstract**: In one embodiment, a system and a method involve receiving a raw signal collected by a sensor that pertains to a temporal trend, creating a reference signal of a known amplitude and frequency, adding the reference signal to the raw signal to form a modulated signal, decomposing the modulated signal to obtain a decomposed signal, and conducting time-frequency analysis on the decomposed signal to detect abnormal patterns.

SYSTEMS AND METHODS FOR DETECTING SMALL PATTERN CHANGES IN SENSED DATA

Cross-Reference to Related Application(s)

This application claims priority to co-pending U.S. Provisional Application serial number 61/489,855, filed May 25, 2011, which is hereby incorporated by reference herein in its entirety.

Background

Sensors are often used to obtain data that is useful in evaluating a system or a situation. For example, it may be desirable to use sensors to monitor the movement of a retaining wall for any indication that the wall is at risk of toppling. As another example, it may be desirable to use sensors to detect the formation of ice on the surface of a road. In such situations, the sensed data can be analyzed and conclusions can be drawn from the analysis.

In certain circumstances, it is difficult to identify the data that is needed to draw conclusions about a system or situation because of other data in the signal. For example, in the case of the retaining wall monitoring, it may be difficult to identify the effect of precipitation on the retaining wall because the effects of temperature expansion are so much greater in magnitude. In the case of the ice formation detection, it may be difficult to detect precipitation on a road surface because the effects of ambient temperature change are so much greater in magnitude. In both situations, small pattern changes are difficult to identify due to the presence

of substantial environmental effects, which act as noise that conceals the small pattern changes.

From the above discussion, it can be appreciated that it would be desirable to have a system or method that can be used to detect such small pattern changes in sensed data.

Brief Description of the Drawings

The present disclosure may be better understood with reference to the following figures. Matching reference numerals designate corresponding parts throughout the figures, which are not necessarily drawn to scale.

Fig. 1 is a flow diagram of an embodiment of a method for performing an auto-modulating pattern (AMP) process.

Fig. 2 is a diagram that illustrates the detectability of an anomalous event of interest using time-frequency analysis.

Figs. 3(a)-(d) are graphs of sample signals used in a parametric study.

Figs. 4(a)-(d) are graphs that compare mode mixing with and without the AMP process.

Fig. 5 is a diagram that illustrates the amplitude and length of edge error.

Figs. 6(a) and 6(b) are diagrams that illustrate the effects of frequency on the amplitude and length of the edge error.

Fig. 7 is a graph that plots tilt time histories measured at three locations: the top, middle, and bottom of a retaining wall.

Figs. 8(a)-(f) are diagrams that illustrate the results of the various steps of an example AMP process.

Figs. 9(a)-(f) are diagrams that illustrate example monotonic and multitonic sinusoidal signals that can be used as a reference signal in the AMP process.

Fig. 10 is a block diagram of an embodiment of an AMP sensor.

Fig. 11 is a schematic drawing of an in-house sensor cluster unit used in a highway pavement field test.

Figs. 12(a)-(e) are temperature versus time plots obtained using temperature sensors shown in Fig. 11.

Figs. 13(a)-(f) are diagrams that illustrate the results of AMP analysis performed in relation to a pavement icing field study.

Fig. 14 is a block diagram of an embodiment of a computing device that can be used to performed AMP detection.

Detailed Description

As described above, it would be desirable to have a system or method that can be used to detect small pattern changes in sensed data. Disclosed herein are examples of such systems and methods. In some embodiments, the systems and methods employ auto-modulating pattern (AMP) detection. As is described below, AMP detection is particularly useful in detecting small but important information that is usually obfuscated by other information, such as environment-related information. In some embodiments, the AMP detection is performed using an AMP sensor that can transmit raw and/or processed data can be used to identify a dangerous an emergency condition, such as vulnerability of a retaining wall or the formation of ice on a roadway.

In the following disclosure, various system and method embodiments are described. It is to be understood that those embodiments are merely example implementations of the disclosed inventions and that alternative embodiments are possible. All such embodiments are intended to

fall within the scope of this disclosure.

Empirical Mode Decomposition

The Empirical Mode Decomposition (EMD) method is a data processing technique developed to deal with nonlinear non-stationary signals. EMD is widely used in science and engineering when time-dependent natural phenomena is to be studied, such as meteorology, atmospheric physics, and seismology. An arbitrary time-dependent signal $x(t)$ can be expressed as a series expansion of *m*-number of intrinsic mode functions (IMFs) that represent oscillatory modes combined in $x(t)$:

$$x(t) = \sum_{k=1}^{m} \mathrm{IMF}_k + r(t) \qquad (1)$$

where $r(t)$ is the residual. The IMF is defined to have local zero means and the same number of zero crossings and extrema. The decomposition of $x(t)$ into IMFs is called the sifting process, and several sifting algorithms have been developed.

The Hilbert-Huang Transform (HHT) method is a time-frequency analysis technique combined with the EMD method. Let $x_k^I(t) = \mathrm{IMF}_k$, then the corresponding analytical signal is defined as

$$z_k^j(t) = x_k^j(t) + iy_k^j(t) = a(t)e^{i\theta(t)} \tag{2}$$

where

$$y_k^j(t) = \frac{1}{\pi} P \int_{-\infty}^{\infty} \frac{x(\tau)}{t-\tau} d\tau \tag{3}$$

$$a(t) = \sqrt{x_k^j(t)^2 + y_k^j(t)^2} \tag{4}$$

$$\theta(t) = \tan^{-1} \frac{y_k^j(t)}{x_k^j(t)} \tag{5}$$

and P is the Cauchy principal value. It should be noted that $y_k^j(t)$ is the convolution of $x_k^j(t)$ with $1/\tau$ that is sensitive to the local properties of $x_k^j(t)$. In addition, the time-dependent functions, $a(t)$ and $\theta(t)$, provide the best local fit of $x_k^j(t)$. The instantaneous frequency can be determined as

$$\omega(t) = \frac{d\theta(t)}{dt} \tag{6}$$

Auto-Modulating Pattern (AMP) Detection

Auto-modulating pattern (AMP) detection is a novel data processing technique that is an extension of the EMD-HHT method and can be used to detect an event of interest whose signature is overshadowed by other various dominant effects entangled together in nonlinear non-stationary signals. AMP detection is particularly useful in field monitoring applications to detect the occurrence of anomalous events under significant (and possibly unknown) environmental variations.

The AMP process described below utilizes a unique property of EMD known-as mode mixing. Because EMD traces the highest frequency components in a given signal locally, the presence of intermittence distorts the shape of the current IMF and subsequent sifting process. Consequently, different modes of oscillations coexist in a single IMF. The effect of mode mixing due to intermittence is significant in EMD because its basis functions (i.e., IMFs) are determined "empirically" from given data. For the same reason, the mode mixing effect is less significant in time-frequency analysis methods using predetermined basis functions, such as the wavelet transform.

Mode mixing is considered an undesirable characteristic of EMD in many applications where deterministic and theoretical decomposition results are required, and numerous techniques have been developed to reduce this effect. In the AMP process, however, the mode-mixing phenomenon is utilized as a necessary property of EMD, instead of being avoided, to improve the detectability of subtle pattern changes in complex non-stationary signals. An arbitrary signal $x(t)$ can be expressed as

$$x(t) = e(t) + m(t) \tag{7}$$

where $e(t)$ is event signal, and $m(t)$ is masking signal. In many field monitoring applications, $m(t)$ is usually the combination of time-dependent variation affected by numerous environmental factors (e.g., structural behavior due to daily and seasonal ambient temperature variation), and $e(t)$ is a very small intermittent event of interest (e.g., structural behavior due to damage). Thus, the goal of the AMP process is (i) to detect the occurrence of event, $e(t)$, which is masked by the dominant component of $m(t)$ in the non-stationary signal of $x(t)$, and (ii) to determine the occurrence time with high temporal accuracy.

In the AMP process, the arbitrary signal $x(t)$ is modulated with a user-defined modulating sinusoidal signal, $\mu^*(t)$:

$$x^*(t) = e(t) + m(t) + \mu^*(t) \tag{8}$$

where $x^*(t)$ is the modulated signal of $x(t)$, and the superscript * denotes user-defined modulation. Due to mode mixing, the IMF closest to the original $\mu^*(t)$, i.e., $\mathrm{IMF}(\mu^*)$, would be

affected with the intermittence of $s(t)$ in the sifting process, so that the occurrence of $s(t)$ could be detected after the time-frequency analysis of the $IMF(\mu^*)$ using the HHT.

The AMP process can be summarized as first modulating $x(t)$ with the user-defined signal, $\mu^*(t)$; then decomposing the modulated signal, $x^*(t)$, using the EMD to find the $IMF(\mu^*)$; and finally performing HHT to detect the intermittence effect of $s(t)$ in the time-frequency plot of the $IMF(\mu^*)$. Fig. 1 is a flow diagram of an example AMP process.

Beginning with block 10 of Fig. 1, a reference signal having a known amplitude and frequency is created. Various mathematical functions can be selected for the reference signal. Example reference signals include sinusoidal, sine-sweep, beating, square, sawtooth, or broadband random functions. The reference signal that is most preferable may depend upon the underlying application. In addition, the amplitude and frequency of the reference signal can be selected depending upon the application. Example reference signals are shown in Fig. 9. Regardless of what type of reference signal is used, the length (in terms of the number of data points) of the reference signal should be the same as the raw signal.

Referring next to block 12, a raw signal is collected. The raw signal can be collected using various types of sensors. Examples of sensors that can be used include displacement sensors, velocity sensors, acceleration sensors, strain sensors, slope sensors, temperature sensors and the like.

Next, the reference signal is added to or mixed with the raw signal to create a modified signal, as indicated in block 14. The mixing can be achieved using a hardware (physical)

approach or a software (synthetic) approach. In the hardware approach, the sensor readings can be physically modulated with a mechanical actuator or motor whose motion is controlled with the reference signal. In the software approach, the reference signal is synthetically mixed with the raw sensor signal with a computer using an appropriate software program. Because the selection of the optimal reference signal for the given raw signal depends upon the underlying application, multiple reference signals with different amplitudes and frequencies can be mixed with the raw signal in parallel, and each modulated signal can be processed separately to maximize the efficiency of the analysis.

With reference next to block 16, the modulated signal is decomposed into multiple decomposed signals. In some embodiments, the decomposition is performed using a non-stationary decomposition technique, such as the wavelet decomposition method (WDM) or the empirical mode decomposition (EMD). Once the decomposition has been performed, a decomposed signal whose frequency is close to the reference signal frequency is selected, as indicated in block 18.

Referring next to block 20, time-frequency analysis is conducted on the selected decomposed signal to detect abnormal patterns. The occurrence of abnormal patterns in the raw signal can be detected as peaks. In some embodiments, the time-frequency analysis is performed using the wavelet transform (WT) or the Hilbert-Huang transform (HHT). The baseline frequency of the selected decomposed signal should be near the frequency of the reference signal in the time-frequency plot.

Turning to block 22, any detected abnormal events are interpreted. In some embodiments, physical interpretation of the abnormal events can be made using additional information of the structures where the raw signal was measured.

The AMP process described above improves the detectability of anomalous event occurrence by "amplifying" small effects of $s(t)$ masked by dominant $m(t)$ in the following two ways: (i) signal-to-noise ratio (SNR), and (ii) temporal resolution of detection. As illustrated in Fig. 2, the SNR can be improved by increasing the peak magnitude of the event and/or reducing the fluctuation of the baseline frequency. In the AMP process, the user-defined sinusoidal signal, $\mu^n(t)$, lays the flat baseline in the time-frequency plot. The temporal resolution also can be improved using a higher frequency of $\mu^n(t)$ than the frequency of $m(t)$; thus the peak width in Fig. 2 would be reduced.

Parametric Study

The peak magnitude and width shown in Fig. 2 largely depends on the amplitude and frequency of $\mu^n(t)$. Thus, a series of parametric studies were conducted to find the optimal characteristics of $\mu^n(t)$.

The following three stopping criteria of the sifting algorithm were used in the EMD process:

1. At each point (mean_amplitude) < THREASHOLD2 * (envelope_amplitude)
2. Mean of Boolean array {(mean_amplitude)/(envelope_amplitude) > THRESHOLD} < TOLERANCE
3. |# zeros - # extrema| ≤ 1

where THRESHOLD = 0.05, THRESHOLD2 = 0.5, and TOLERENCE = 0.05 for all weather

chamber data sets used in the study. The maximum iteration of the sifting process was set to be 2000.

A first parametric study was conducted using two types of masking signals as

$$m(t) = m_p(t) + m_a(t) \tag{9}$$

where $m_p(t)$ was a sinusoidal signal simulating a periodic environmental variation (e.g., yearly fluctuation of air temperature), and $m_a(t)$ was a sigmoid signal simulating long-term drift of $m(t)$ (e.g., air temperature drifting over multiple years). The modulating signal, $\mu^*(t)$, was chosen to be a sinusoidal signal with a higher frequency than the frequency of $m(t)$. A sample set of signals used in the parametric study is shown in Fig. 3. In particular, Fig. 3(a) shows a periodic masking signal, $m_p(t)$, Fig. 3(b) shows a drifting masking signal, $m_a(t)$, Fig. 3(c) shows a masking signal, $m(t) = m_p(t) + m_a(t)$, and Fig. 3(d) shows a modulated signal, $m^*(t) = m(t) + \mu^*(t)$.

The above synthetically generated signals were processed using the EMD method with and without modulating signals. Fig. 4(a) shows the original $m_p(t)$ and resulting $\mathrm{IMF}(m_p)$ without modulation using $\mu^*(t)$, and Fig. 4(c) shows the error between those two signals. The

error shows that the $IMF(m_p)$ is interfered over time by the other masking signal, $m_a(t)$, due to mode mixing. To increase the detectability, it is desired that the $IMF(m_p)$ is not mode-mixed with $m_a(t)$, but with $s(t)$.

The mode-mixing effect in the $IMF(m_p)$ can be significantly reduced with the frequency modulation using $\mu^*(t)$. Fig. 4(b) shows the $\mu^*(t)$ and corresponding IMF of $\mu^*(t)$, and the error between those two signals is shown in Fig. 4(d). The error between the time range of 0.1 and 0.9 is almost zero and implies the interference by $m_a(t)$ becomes negligible in this time range. The interference reduction is because the frequency of $\mu^*(t)$ is further from the frequency of $m_a(t)$ than that of $m_p(t)$. In Fig. 4(d), however, the error is concentrated near the edges. This phenomenon is own as edge effect. Since the edge effect is influenced by $\mu^*(t)$, the parametric study was further conducted on the amplitude and frequency of $\mu^*(t)$ to minimize the edge effect.

The comparison in Fig. 4 illustrates the advantage of the AMP process with improved detectability by reducing error due to interference with the other masking signal in the middle section. The errors near the edges are due to the edge effect of the EMD. The parametric study was further conducted to investigate the effects of the frequency and amplitude of the modulating signal, $\mu^*(t)$.

The influence of the frequency modulation on the edge effect was investigated for different frequencies of $\mu^*(t)$. The edge effect was measured in two ways: the amplitude and length of the edge error, $e = \mathrm{IMF}(\mu^*) - \mu^*(t)$, as shown in Fig. 5.

In the parametric study, the modulating frequency was selected to be larger than the frequency of the periodic masking signal, $m_3(t)$, which is the frequency of 3 as shown in Fig. 3(a). The results of the parametric study on the edge effects for different modulating frequencies are shown in Fig. 6(a), which illustrates the edge error amplitude, and Fig. 6(b) which illustrates the edge error length. For the comparison, the edge errors of amplitude and length were normalized to the errors at the frequency of 4, which was the lowest tested frequency. Both the edge error amplitude and length decayed exponentially as the modulating frequency increased. The decaying rate of frequency was measured using the least square estimation: 4.5 for the normalized edge error amplitude, and 3.9 for the normalized edge error length. Consequently, both normalized edge errors were reduced to approximately 10% at the frequency of 45 for the window length of 1.

Retaining Wall Application

The usefulness of the AMP process was evaluated in a case study performed using a full-scale reinforced concrete retaining wall that is 13.59 meters (m) tall. The material properties of the reinforced concrete and backfilled soil were unknown. Because the wall was placed only 9.5 m away from a high-rise residential apartment building, the collapse of the wall would result in a

catastrophic disaster.

The retaining wall was monitored for three years with three tilt sensors located at the top, middle, and bottom of the wall. Three tilt gauges were mounted on the wall surface at 1.68 m, 6.55 m, and 13.14 m from the ground to measure the wall slope at each location. At the same locations of the tilt gauges, the surface temperatures were also measured. The sensor readings were sampled once every hour (1 sample/hour) for all channels using a digitizer and local storage device. Although wall surface temperature data were collected, only tilt data were used in the analysis to demonstrate that important information can be obtained using response-only data without relying on additional data of causative force and environmental factors in modeling process.

The tilt time histories measured from the retaining wall are shown in Fig. 7. The slope is in micro-radians (slope towards the apartment side is positive). As can be appreciated from Fig. 7, the slope signals at all three locations were significantly affected by seasonal and daily variation: decreasing during summer and increasing during winter, and decreasing during days and increasing during nights as reflected in daily trends (not shown in the figure). During the three-year monitoring period, the wall behavior was affected by temperature change in addition to rain and snow falls, free-thaw of backfilled soil, soil-structure interaction, and the like. Fig. 7 shows the complexity of the problem and how difficult it is to obtain important performance-related information out of a very limited amount of the raw sensor data.

Fig. 7 also shows that the collected sensor data are partially incomplete. The bottom sensor failed in Q1 of 2006 (approximately after one year). In addition, there were "missing" data for all sensors in Q4 of 2006 for about three months due to instrument failure. These unavoidable and unpredictable sensor and instrumentation problems are frequently encountered

in long-term field measurements, and the proposed non-parametric methodology should be robust enough to handle these kinds of problems.

Precipitation is the most important environmental factor in the operation of retaining walls: rain and snow falls increase the water content, the weight of the backfilled soil, and the pore-water pressure. Because high pore-water pressures can cause the collapse of retaining walls, excessive water in the backfilled soil must be drained out properly.

The AMD process was used to process the field measurements and the results are summarized in Fig. 8. Fig. 8(a) shows raw signals that were collected with a tilt gauge. Fig. 8(b) shows a reference signal of known amplitude and frequency that was created. In this example, a monotonic sinusoidal function with the frequency of two per day was selected. Examples of reference signals other than sinusoidal signals that can be used include sine-sweep, square, sawtooth, and broadbank random signals. Fig. 9 shows examples of monotonic and multitonic sinusoidal signals that can be used as a reference signal.

Fig. 8(c) shows a modulated signal that results from the combination of the raw signal (Fig. 8(a)) with the reference signal (Fig. 8(b)). The two signals can be combined using either the hardware approach or software approach, as described above. Fig. 8(d) shows the result after disentangling the signal whose frequency is close to that of the reference signal from the modulated signal. In this example, the signal with the frequency near two per day has been decomposed using EMD. That frequency is the frequency of the reference signal in Fig. 8(b). Fig. 8(e) shows the result of time-frequency analysis to detect abnormal patterns. In this example, HHT was used, although other time-frequency analysis techniques, such as the wavelet transform, can be used. The baseline frequency in Fig. 8(e) is at two per day, which is the same as the reference signal frequency. Abnormal patterns, as compared to the baseline frequency, are

identified by the peaks in the figure. Finally, Fig. 8(f) shows the result of interpreting the detected abnormal events. In this example, the detected peaks (abnormal events) were caused from the change of the retaining wall motion due to an excessive amount of water in the backfilled soil after precipitation.

As can be appreciated from the above discussion, the accuracy of non-parametric data processing techniques can be even more improved using the AMP process. In the above-described field tests, the daily oscillation in time histories of the sensor measurements was used as the nominal pattern. Although the frequency of the daily trend (mainly due to daily temperature variation) remains mostly at 1/day, the trend is a nonlinear function (i.e., not a perfect sinusoidal function), so that the baseline frequency fluctuates over time. Also, using the daily trend, the frequency of the nominal pattern is limited to a diurnal scale. The pattern detectability can be significantly improved by intentionally mixing the raw sensor signal with a "small" reference signal with known amplitude and frequency.

An advantage of the auto-modulation technique described herein is that users can define the reference signal so that they do not have to rely on reference patterns in natural processes, such as the daily trend discussed in relation to Fig. 8. In some embodiments, the AMP process can be performed by a sensor that includes a data acquisition module, a microprocessor, memory, a data storage unit, a communication unit, and a communication unit, as shown in Fig. 10. Substantially any type of sensor can be used to measure structural response. The sensors are connected to the data acquisition module to digitize the sensor reading. The digitized sensor data can then be processed with the microprocessor using embedded AMP algorithms to detect abnormalities in the structural response. Using the communication unit, the raw and processed data can be transmitted to remote computers or portable devices via wired or wireless

communication protocols. Due to harsh environment at field sites, it may be advisable to protect the embedded computer in a ruggedized container.

Pavement Icing Application

A field test was also performed to see if the intermittent event of rainfall or icing of a pavement surface could be detected despite the presence of dominating environmental fluctuations. These dominating trends, especially the air temperature, significantly complicate both the nature of the problem by making the system response nonlinear and nonstationary, and inhibit the ability to detect the event of interest. In order to achieve this goal, it was necessary to conduct a full-scale experimental study using pavement surface temperature data collected from sensors during in-service traffic conditions.

The location of the field test was on the Donghae Highway pavement, which is located in South Korea. Because the test was close in proximity to the Kangreung tunnel, this test was referred to as "KR5" during the duration of the project. Reliable sensors that were both cheap and efficient were required in order to conduct an experiment of this magnitude. Two different classes of sensors were used for KR5: "contact" and "noncontact." Pavement temperatures at different depths were collected using an RTD 4-Wire "contact" sensor (15 cm diameter). The RTD sensor also included a surface moisture sensor on the top to detect moisture on the road surface. The sensor was secured using the rapid curing MK-Crete 45 concrete mix. Fig. 11 shows a graphical depiction of the embedded sensor used for the field experiment.

Referring to Fig. 11, the level temperature sensors were used to measure pavement temperature at depths of 2 cm, 5 cm, and 8 cm below the pavement surface. Surface sensors were placed at the top to measure temperature and moisture.

Two types of "noncontact" sensors were used for KR5. First, an infra-red camera was mounted and secured using anchor bolts on top of a container to provide real-time camera footage of the pavement surface. The footage retrieved from the camera could be used for validation purposes when compared to the data. The second type of noncontact sensor was used to measure the ambient air temperature and the relative humidity for reference. The data from the sensors described were collected using a data acquisition (DAQ) system.

The data used for the experiment was recorded from November 2011 until March 2012. Fig. 12(a) shows the ambient air temperature for this time period. Figs. 12(c)-(e) show the pavement temperature at different depths, i.e., 0 cm, 2 cm, 5 cm, and 8 cm, respectively. The data was sampled at a rate of one sample per second.

As can be appreciated from Fig. 12, it is very difficult to identify the exact times at which an intermittent rainfall event occurred because the data is nonlinear and nonstationary. Also, one may notice several unnatural trends, particularly during 2011/12/02 to 2011/12/08, 2011/12/27 to 2012/01/13, 2012/02/01 to 2012/02/10, and after 2012/02/16. These unnatural trends represent the periods of time where the sensors stopped working, or when the data was unable to be retrieved. It should be noted that this is common and unavoidable in sensor measurement applications, and that it is critical to process the data using an algorithm that is robust enough to deal with sensor and measurement error.

Because of the extensive amount of data, the data used for the analysis was truncated to an approximately two week time period (from 2012-01-16 to 2012-01-30) in order to save processing time. This action can be justified by the fact that a two week time period possesses enough cycles (peaks and valleys) for EMD to decompose accurately. Furthermore, the data was undersampled from one sample per second to one sample per 30 seconds. Although this action

reduces the sampling rate and therefore the resolution, it is still more than sufficient to describe the case of an abnormal event. As a result of these two actions, an enormous amount of processing time was saved, without reducing the accuracy or integrity of the results.

A representative sample of the pavement surface temperature data was chosen for analysis, and the results are summarized in Fig. 13. The temperature is represented in degrees Celsius (°C). The data was originally sampled at once per second (1 Hz). Due to the significant volume of data, however, the data was undersampled to a sampling rate of one sample per thirty seconds (1/30 Hz) to reduce the processing time. Fig. 13(a) shows the the pavement surface temperature time history (solid line) with approximately two-week duration from 2012/01/16 to 2012/01/31. Significant daily trends, mostly due to air temperature fluctuation, were observed. One interesting phenomenon was also observed between 01/18 and 01/21, where the cyclic trend appears to flatten and much less fluctuation occurs. The air temperature (dashed line) during the same period is presented for comparison purposes. It should be noted that the AMP process was applied to the pavement surface temperature data only, and the air temperature data was not used in the analysis.

The raw surface temperature data in Fig. 13(a) was intentionally mixed with a synthetic sinusoidal modulating signal as per the AMP process, and the modulated signal was obtained, as shown in Fig. 13(b). The frequency of the modulating signal was one cycle per 30 minutes. This frequency was specifically tailored to detect those intermittent pattern changes that occurred within a short time span of 30 minutes as the temporal resolution of the timing of deicing solution spraying. The amplitude of the modulating signal was defined as ±6°C.

The modulated signal was then processed using the EMD method. The IMF corresponding to the user-defined modulating signal was selected with the known frequency and

amplitude. Fig. 13(c) shows the IMF of the modulated signal. The following three stopping criteria of the sifting algorithm were used in the EMD process:

1. At each point, (mean_amplitude) < THRESHOLD2 * (envelope_amplitude)
2. Mean of Boolean array {mean_amplitude/(envelope_amplitude) > THRESHOLD} < TOLERENCE
3. |# zeros - # extrema| ≤ 1

where THRESHOLD = 0.05, THRESHOLD2 = 0.5, and TOLERENCE = 0.05 for all weather chamber data sets used in this study. The maximum iteration of the sifting process was set to be 2000.

Next, the IMF was transformed into the time-frequency domain using the HHT method. Fig. 13(d) shows the instantaneous frequency characteristics corresponding to the IMF of the modulating signal. The result can be confirmed as the baseline frequency coincides with 2 cycles per hour, which is the user-defined frequency of the modulating signal.

Fig. 13(d) is compared with the pavement surface and climate conditions in the same time scale shown in Figs. 13(e) and 13(f), respectively. The surface and climate conditions were identified at every 30 minutes from visual inspection using the video camcorder records. Referring to Fig. 13(e), one can see that the first snow-piled event (P) occurred on 01/21 from 04:00 AM to 05:30 AM. Observing Fig. 13(d), one can find a large peak corresponding to the same time that the snow-piled event occurred. The similar correlation between the peak of Fig. 13(d) and snow-piled event were observed on 01/22 from 06:30 PM to 07:30:00 PM. Thus, these results show that the AMP process can detect the immediate pavement surface pattern change from a wet completely state (WC) to a snow-piled state (P), which is an important information to determine the timing of the deicing solution spraying.

The AMP process was also able to detect the change of the snow-weak event (SW) to snow-strong event (SS) shown in Fig. 13(f) on 01/20 from 10:00 PM to 11:00 PM. In this time period, a prominent peak was observed in Fig. 13(d).

From 1/23, it was observed that the climate condition remained normal. Although there was no wet climate event in this period, Fig. 13(e) showed the pavement condition was identified wet slightly (WS) approximately from the midnight to the midday. It was found that during night the pavement surface was wetted with night dew because of the dropped temperature and the surface dried after sunrise. The surface condition changes from the wet slightly state to the dry state were detected using the AMP process from 1/25 to 1/29.Fig. 14 illustrates an example configuration for a computing device 30 that can be used to perform at least some of the actions described above. As is shown in Fig. 14, the computing device 30 comprises a processing device 32, memory 34, a user interface 36, and at least one I/O device 38, each of which is connected to a local interface 40.

The processing device 32 can includé a central processing unit (CPU) or a semiconductor based microprocessor (in the form of a microchip). The memory 34 includes any one of or a combination of volatile memory elements (e.g., RAM) and nonvolatile memory elements (e.g., hard disk, ROM, tape, etc.). The user interface 36 comprises the components with which a user interacts with the computing device 30, and the I/O devices 38 are adapted to facilitate communications with other devices.

The memory 34 is a non-transitory computer-readable medium and stores programs (i.e., logic) including an operating system 42 and an auto-modulating pattern (AMP) detection algorithm 44 that is adapted to perform an AMP process of the type described above.

CLAIMS

Claimed are:

1. A method for detecting small pattern changes in sensed data, the method comprising:

receiving a raw signal collected by a sensor that pertains to a temporal trend;

creating a reference signal of a known amplitude and frequency;

adding the reference signal to the raw signal to form a modulated signal;

decomposing the modulated signal to obtain a decomposed signal; and

conducting time-frequency analysis on the decomposed signal to detect abnormal patterns.

2. The method of claim 1, wherein receiving raw data comprises receiving displacement data or temperature data from the sensor.

3. The method of claim 1, wherein creating a reference signal comprises creating one of a sinusoidal, sine-sweep, beating, square, sawtooth, or broadband random function.

4. The method of claim 1, wherein adding the reference signal to the raw signal comprises physically modulating a mechanical actuator using the reference signal.

5. The method of claim 1, wherein adding the reference signal to the raw signal comprises synthetically mixing the reference signal with the raw signal using a computer.

6. The method of claim 1, wherein decomposing the modulated signal comprises performing a non-stationary decomposition technique on the modulated signal.

7. The method of claim 6, wherein the non-stationary decomposition technique comprises wavelet decomposition (WD) or empirical mode decomposition (EMD).

8. The method of claim 1, wherein conducting time-frequency analysis comprises processing the decomposed signal using Hilber-Huang transformation (HHT).

9. The method of claim 1, further comprising interpreting the detected abnormal events.

10. A non-transitory computer-readable medium that stores an auto-modulating pattern (AMP) detection algorithm, the computer-readable medium comprising:

logic configured to add a reference signal of a known amplitude and frequency to a raw signal collected by a sensor to form a modulated signal;

logic configured to decompose the modulated signal to obtain a decomposed signal; and

logic configured to conduct time-frequency analysis on the decomposed signal to detect abnormal patterns.

11. The computer-readable medium of claim 10, wherein the logic configured to add a reference signal is configured to add one of a sinusoidal, sine-sweep, beating, square, sawtooth, or broadband random function to the raw signal.

12. The computer-readable medium of claim 10, wherein the logic configured to add the reference signal is configured to synthetically mix the reference signal with the raw signal.

13. The computer-readable medium of claim 10, wherein the logic configured to decompose the modulated signal comprises logic configured to perform a non-stationary decomposition technique.

14. The computer-readable medium of claim 13, wherein the logic configured to perform non-stationary decomposition technique comprises logic configured to perform wavelet decomposition (WD) or empirical mode decomposition (EMD) on the modulated signal.

15. The computer-readable medium of claim 10, wherein the logic configured to conduct time-frequency analysis comprises logic configured to process the decomposed signal using Hilber-Huang transformation (HHT).

16. The computer-readable medium of claim 10, further comprising logic configured to interpret the detected abnormal events.

17. An auto-modulating pattern (AMP) sensor, comprising:

a sensor element adapted to measure an environmental parameter;

a processing device that is embedded with an AMP detection algorithm, the algorithm being configured to add a reference signal of a known amplitude and frequency to a raw signal

collected by the sensor to form a modulated signal, to decompose the modulated signal to obtain a decomposed signal, and to conduct time-frequency analysis on the decomposed signal to detect abnormal patterns.

18. The sensor of claim 17, wherein the sensor element is configured to measure displacement.

19. The sensor of claim 17, wherein the sensor element is configured to measure temperature.

20. The sensor of claim 17, further comprising a communication unit with which the sensor can communicate data to a remote computing device.

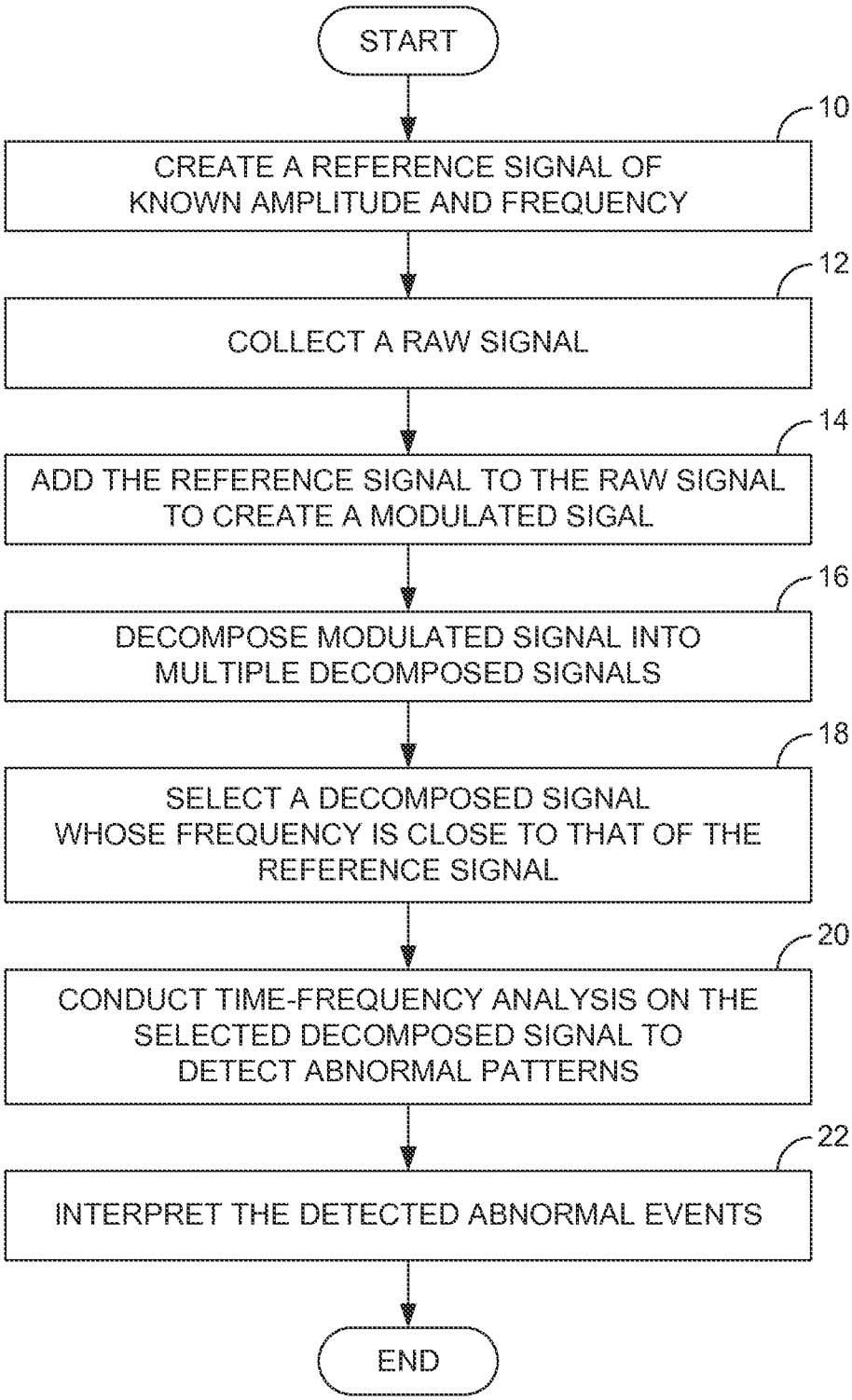
START
10
CREATE A REFERENCE SIGNAL OF KNOWN AMPLITUDE AND FREQUENCY
12
COLLECT A RAW SIGNAL
14
ADD THE REFERENCE SIGNAL TO THE RAW SIGNAL TO CREATE A MODULATED SIGAL
16
DECOMPOSE MODULATED SIGNAL INTO MULTIPLE DECOMPOSED SIGNALS
18
SELECT A DECOMPOSED SIGNAL WHOSE FREQUENCY IS CLOSE TO THAT OF THE REFERENCE SIGNAL
20
CONDUCT TIME-FREQUENCY ANALYSIS ON THE SELECTED DECOMPOSED SIGNAL TO DETECT ABNORMAL PATTERNS
22
INTERPRET THE DETECTED ABNORMAL EVENTS
END

FIG. 1

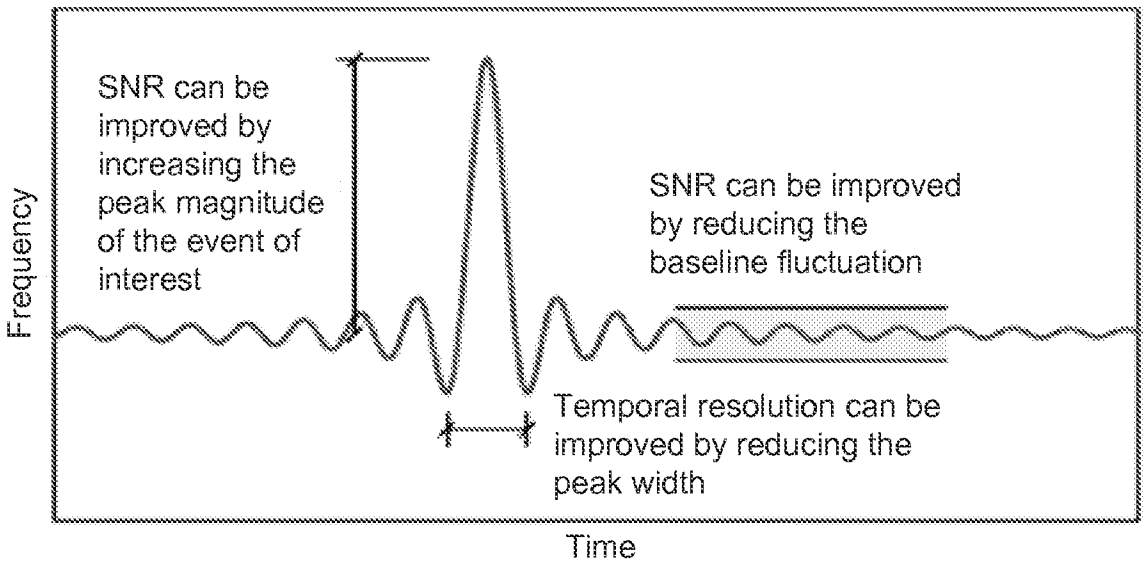
SNR can be improved by increasing the peak magnitude of the event of interest
SNR can be improved by reducing the baseline fluctuation
Temporal resolution can be improved by reducing the peak width
Frequency
Time

FIG. 2

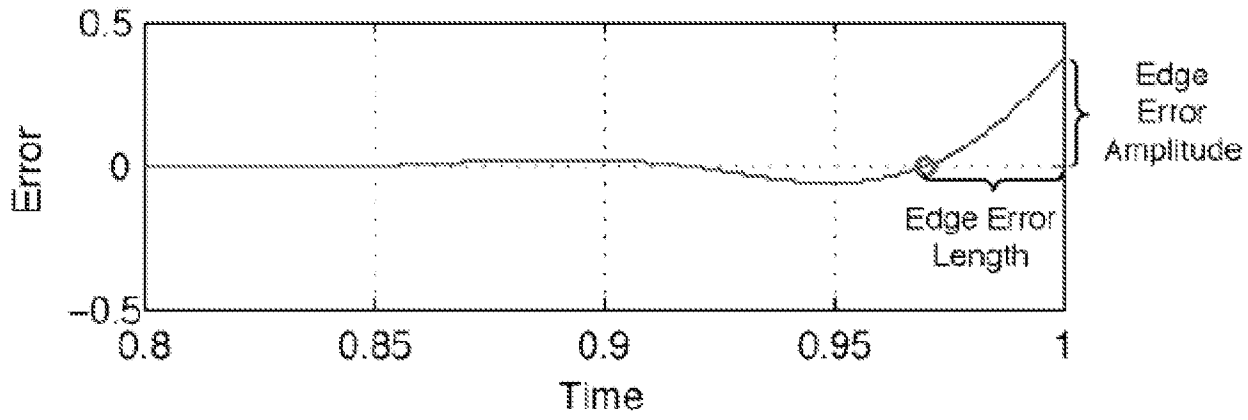
0.5
0
−0.5
Error
0.8
0.85
0.9
0.95
1
Time
Edge Error Amplitude
Edge Error Length

FIG. 5

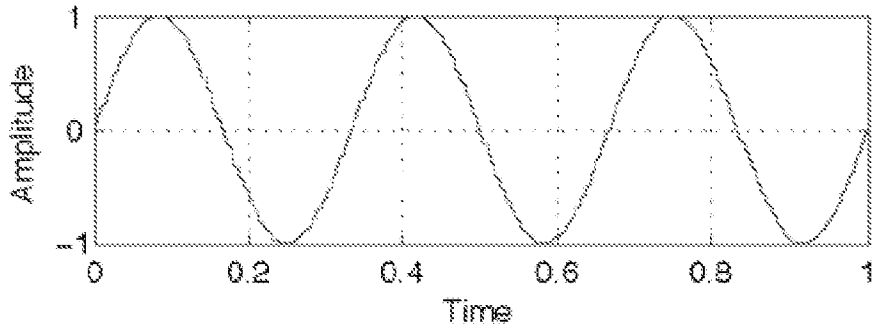

FIG. 3(a)

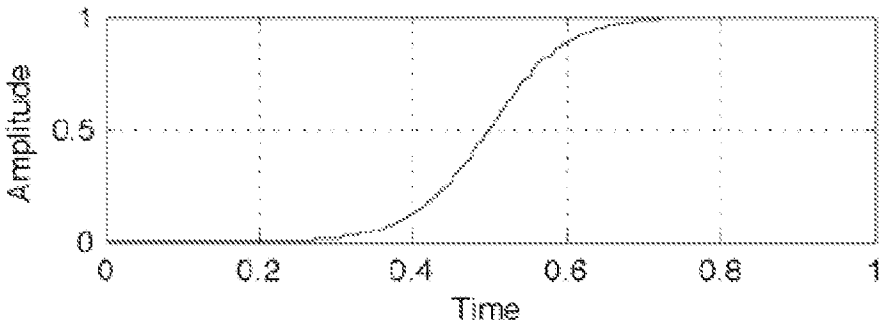

FIG. 3(b)

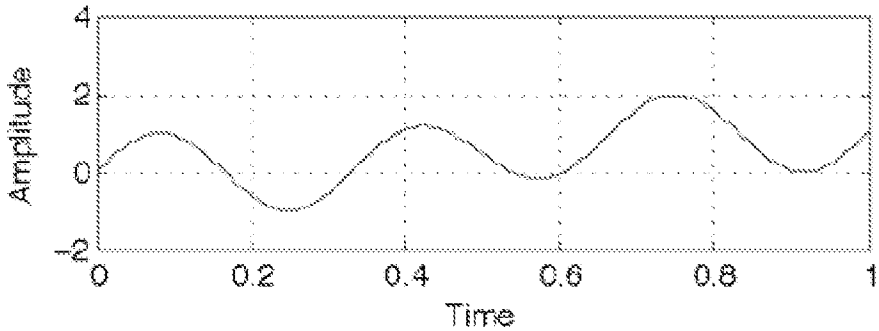

FIG. 3(c)

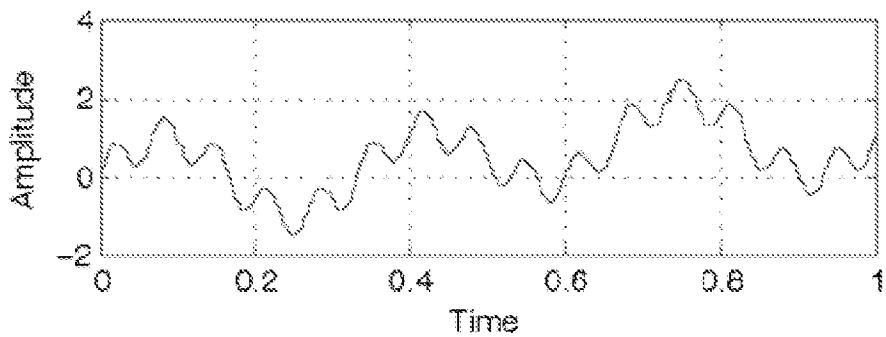

FIG. 3(d)

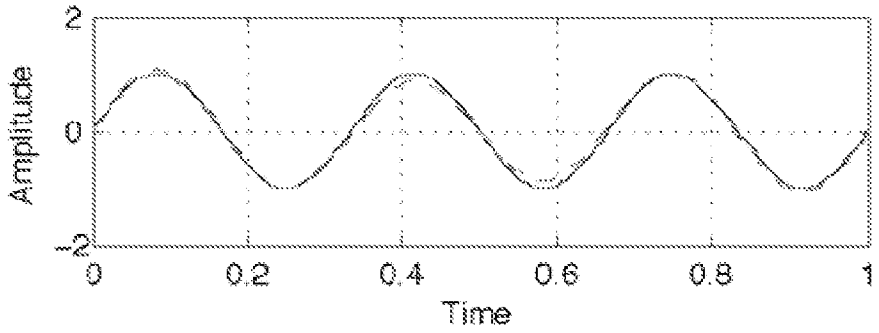

FIG. 4(a)

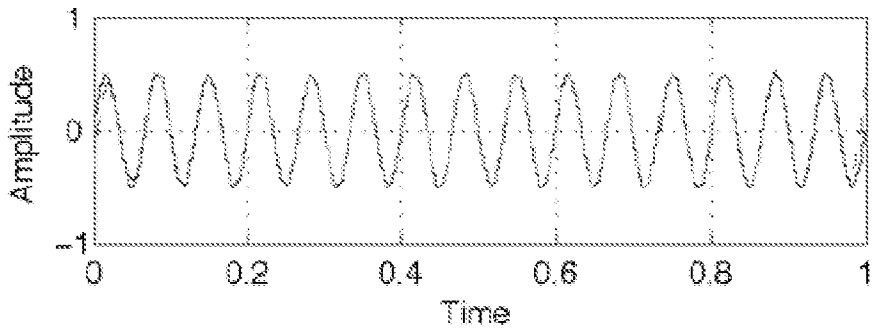

FIG. 4(b)

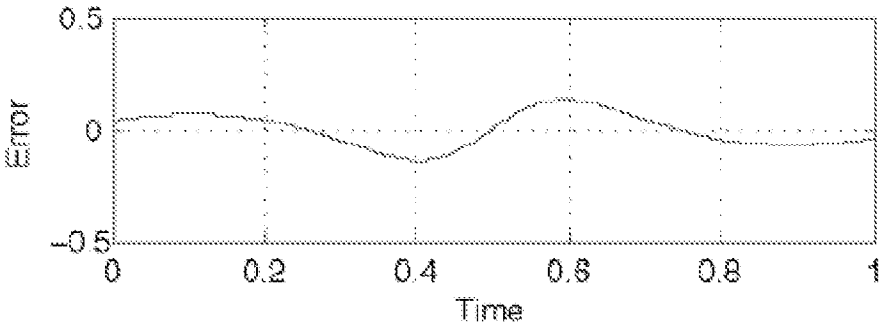

FIG. 4(c)

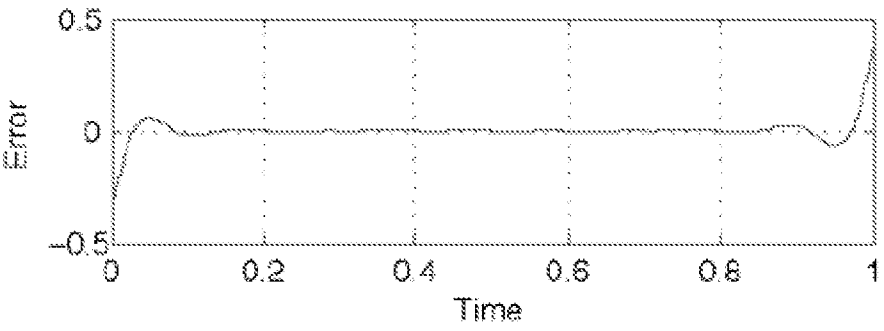

FIG. 4(d)

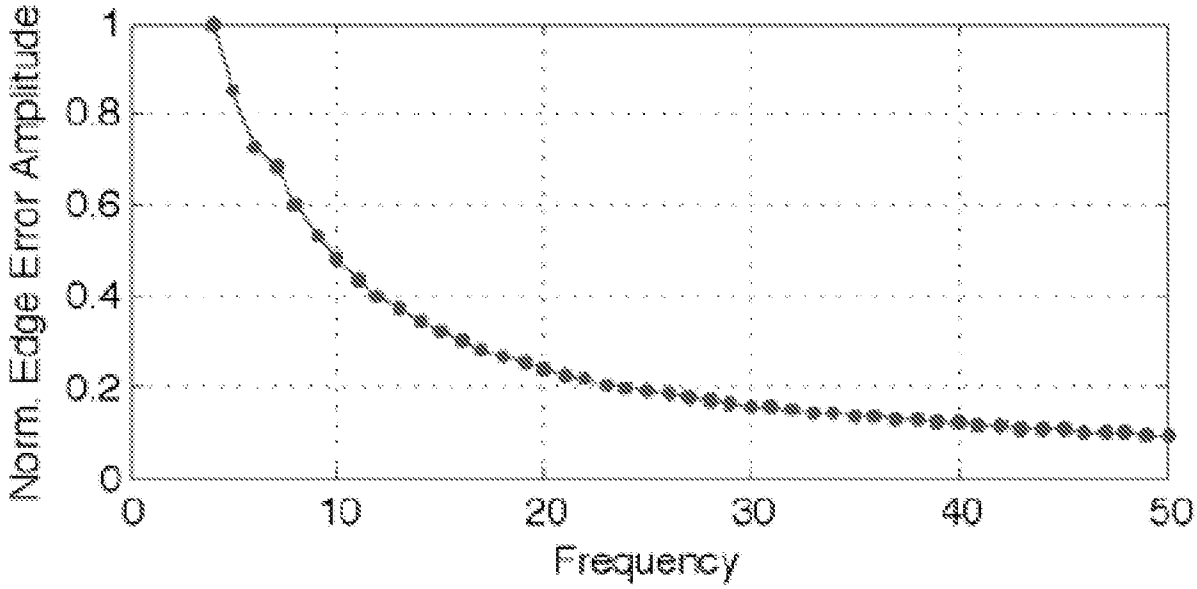
Norm. Edge Error Amplitude
1
0.8
0.6
0.4
0.2
0
0
10
20
30
40
50
Frequency

FIG. 6(a)

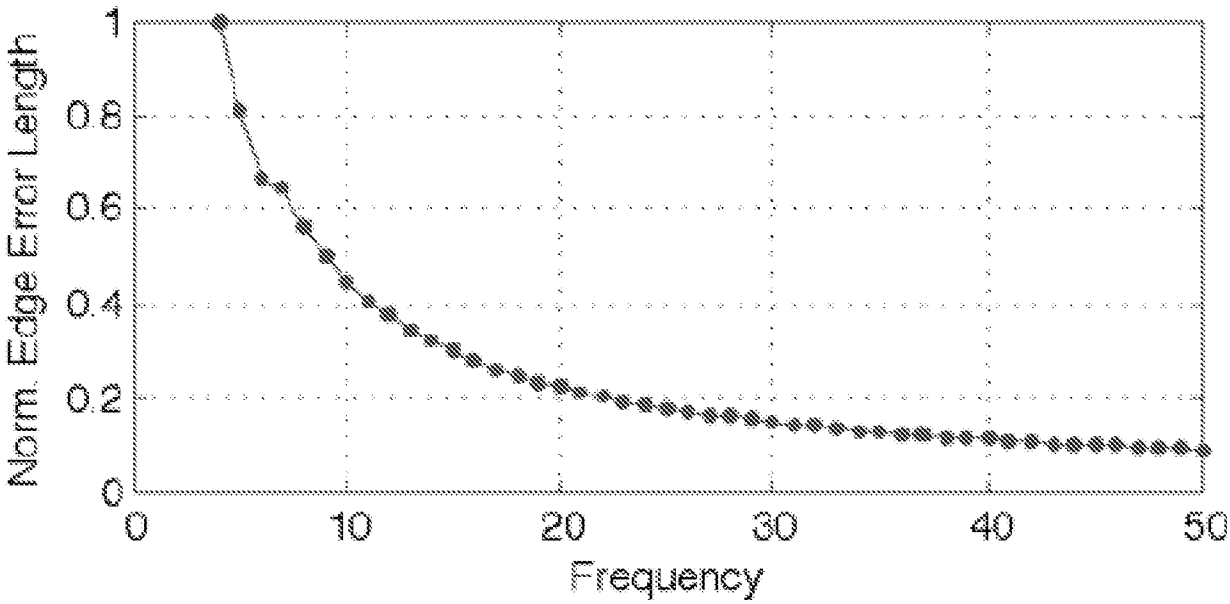
Norm. Edge Error Length
1
0.8
0.6
0.4
0.2
0
0
10
20
30
40
50
Frequency

FIG. 6(b)

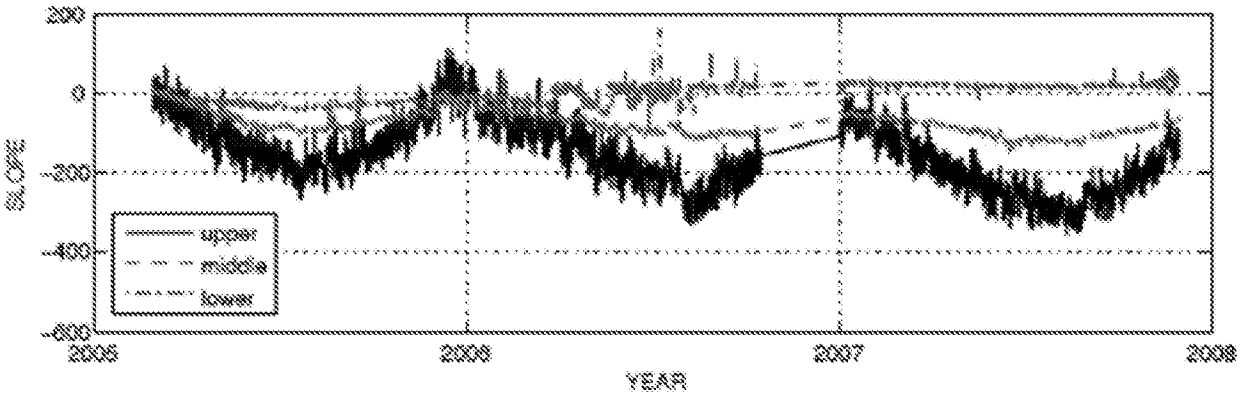
200
0
-200
-400
-600
STRAIN
upper
middle
lower
2006
2006
2007
2008
YEAR

FIG. 7

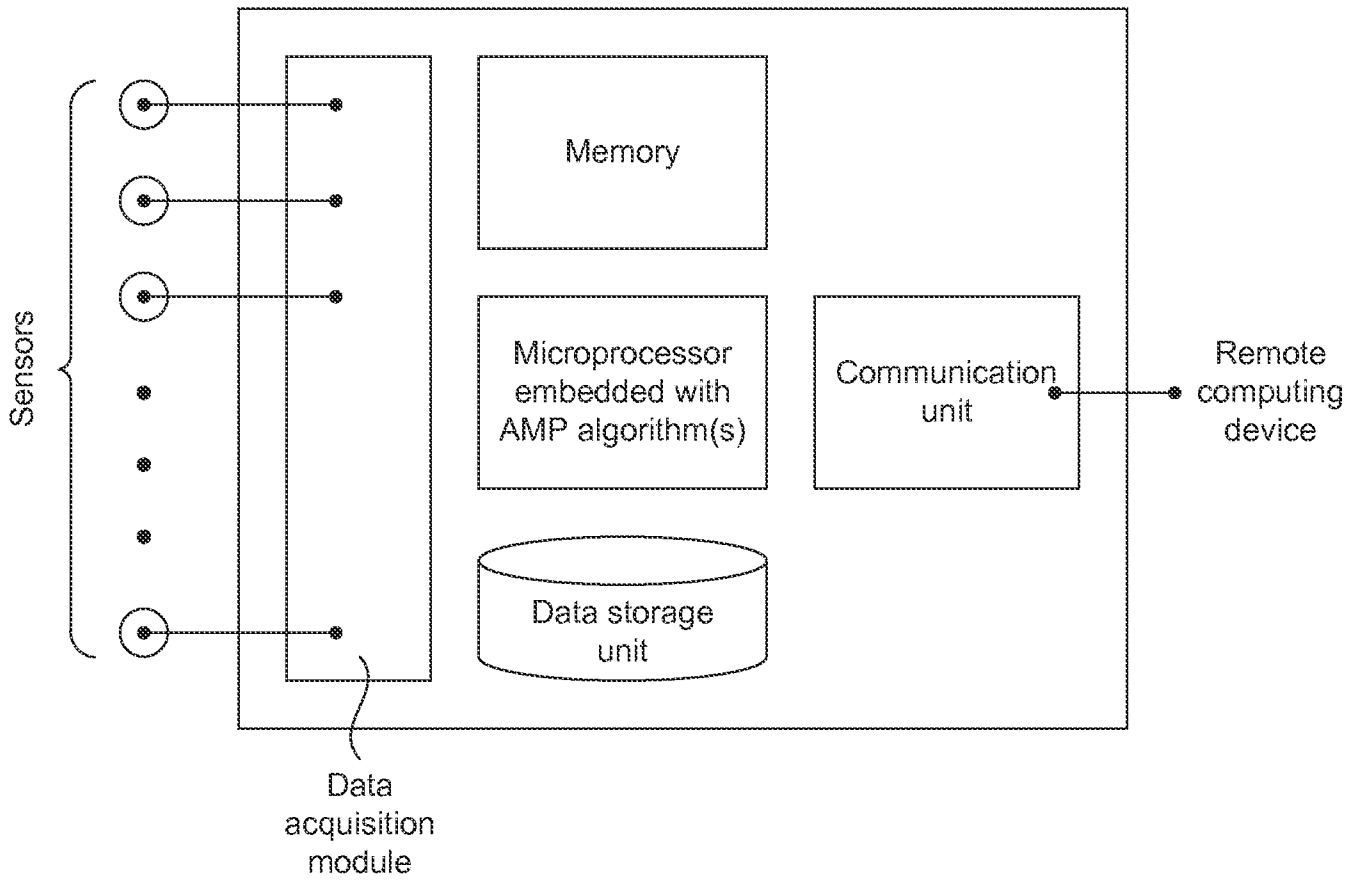
Sensors
Memory
Microprocessor embedded with AMP algorithm(s)
Communication unit
Remote computing device
Data storage unit
Data acquisition module

FIG. 10

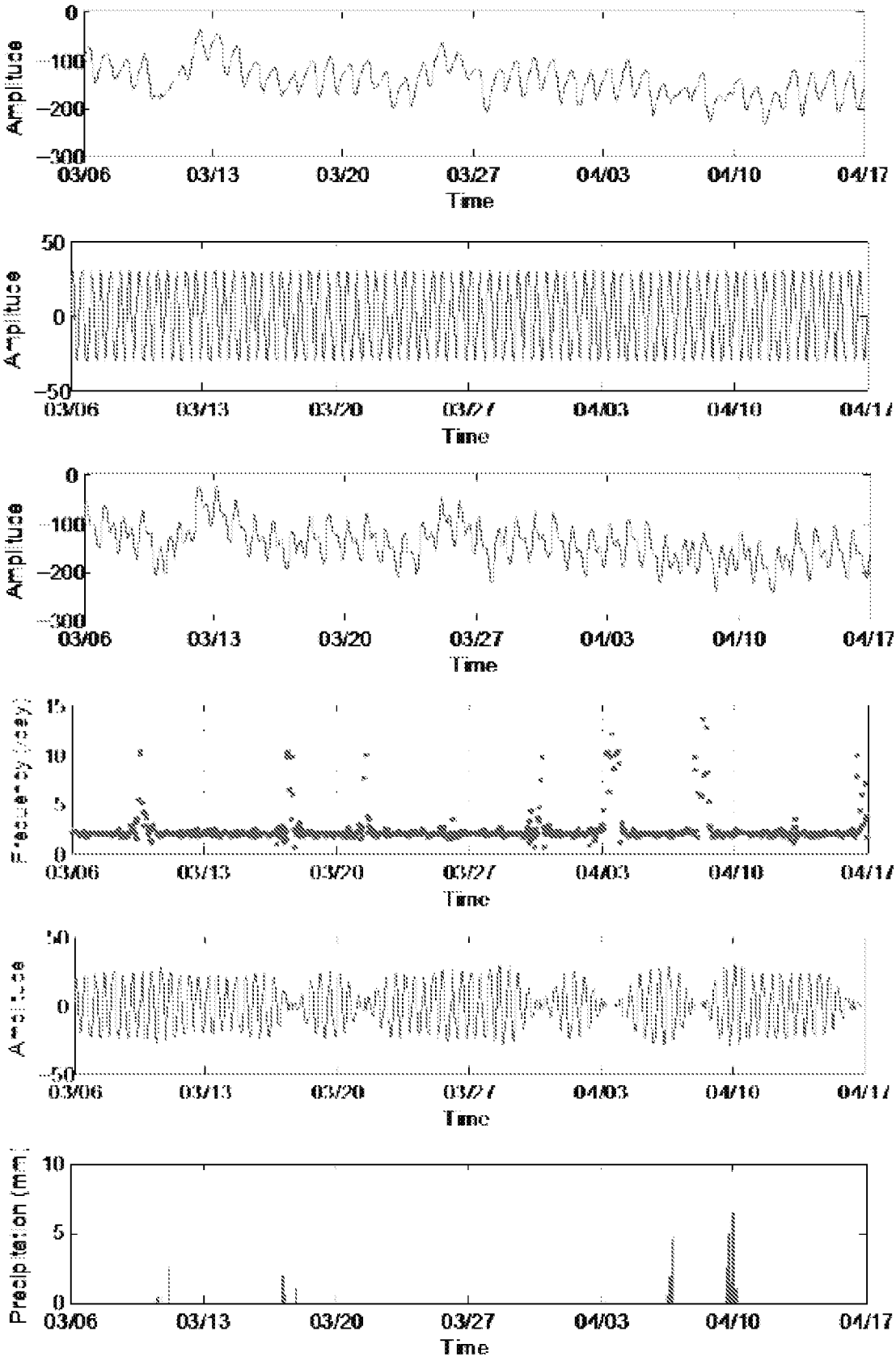
Amplitude
0
−100
−200
−300
03/06
03/13
03/20
03/27
04/03
04/10
04/17
Time
(a)
Amplitude
50
0
−50
03/06
03/13
03/20
03/27
04/03
04/10
04/17
Time
(b)
Amplitude
0
−100
−200
−300
03/06
03/13
03/20
03/27
04/03
04/10
04/17
Time
(c)
10
5
0
03/06
03/13
03/20
03/27
04/03
04/10
04/17
Time
(d)
0
03/06
03/13
03/20
03/27
04/03
04/10
04/17
Time
(e)
Precipitation (mm)
10
5
0
03/06
03/13
03/20
03/27
04/03
04/10
04/17
Time
(f)

FIG. 8

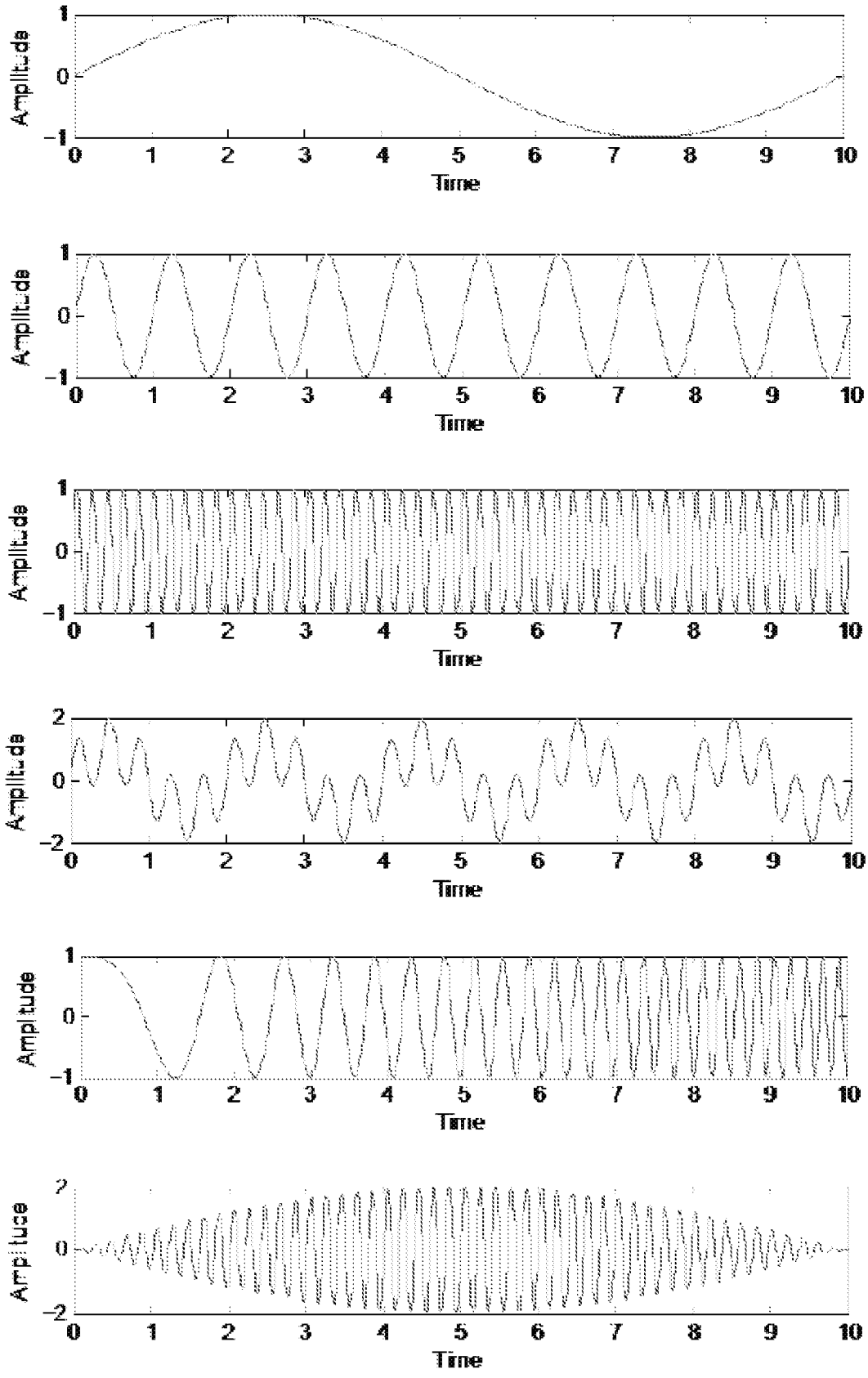

FIG. 9

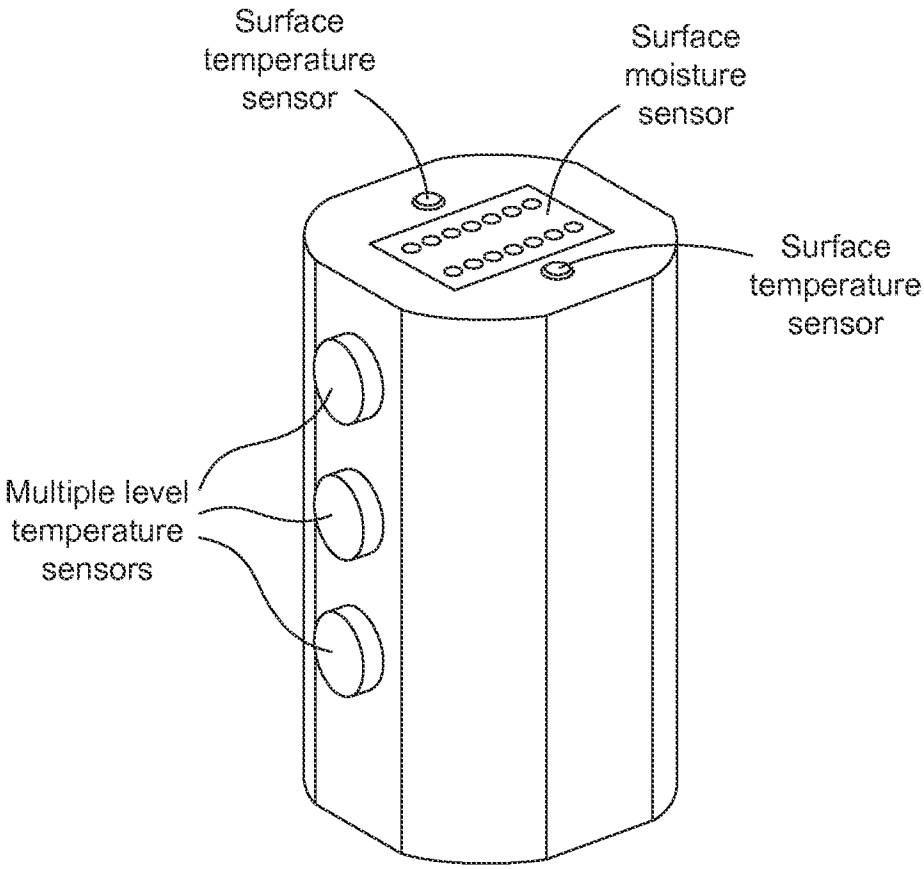
Surface temperature sensor
Surface moisture sensor
Surface temperature sensor
Multiple level temperature sensors

FIG. 11

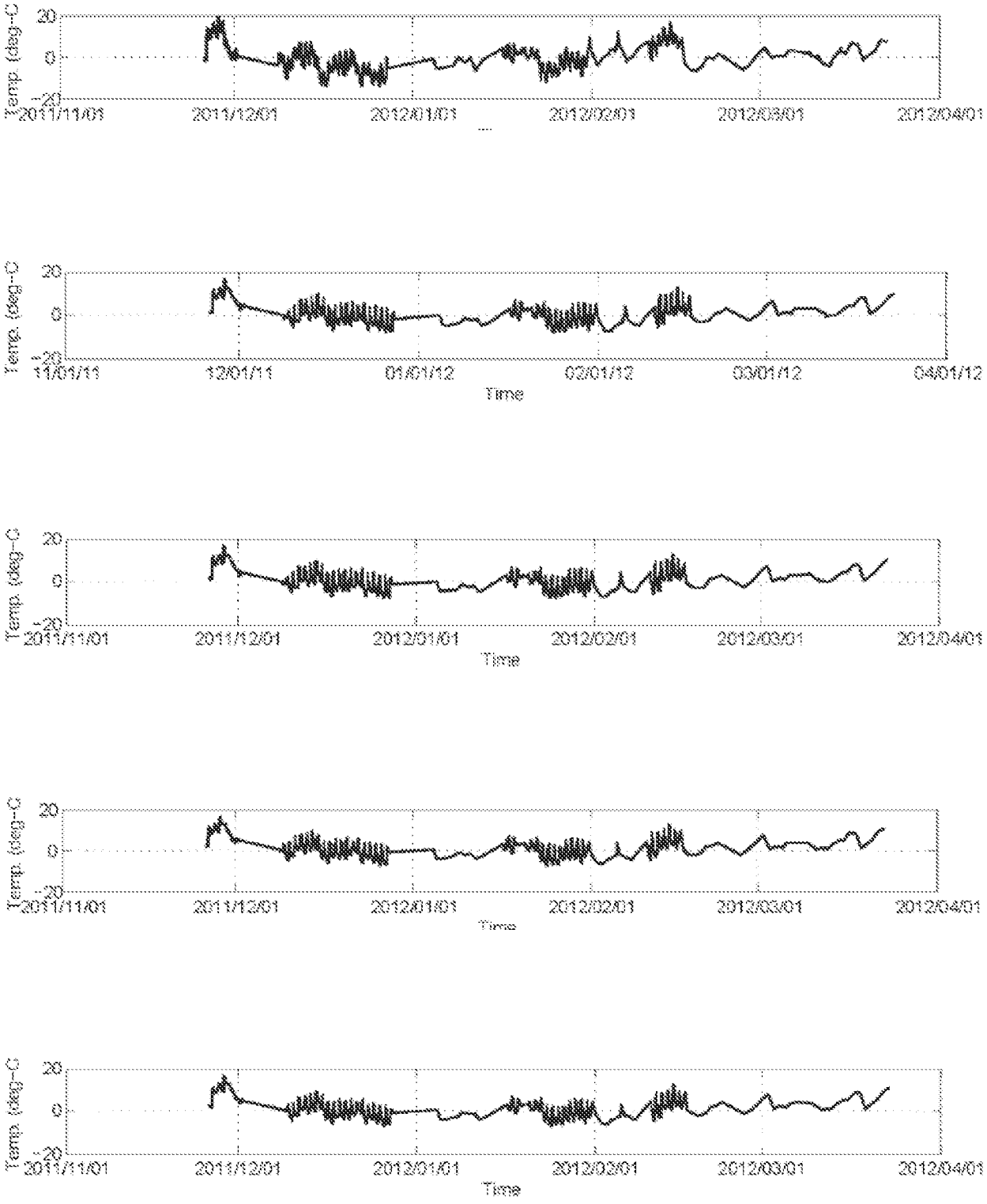
Temp (deg-C)
20
0
-20
2011/11/01
2011/12/01
2012/01/01
2012/02/01
2012/03/01
2012/04/01
(a)
11/01/11
12/01/11
01/01/12
02/01/12
03/01/12
04/01/12
Time
(b)
(c)
(d)
(e)

FIG. 12

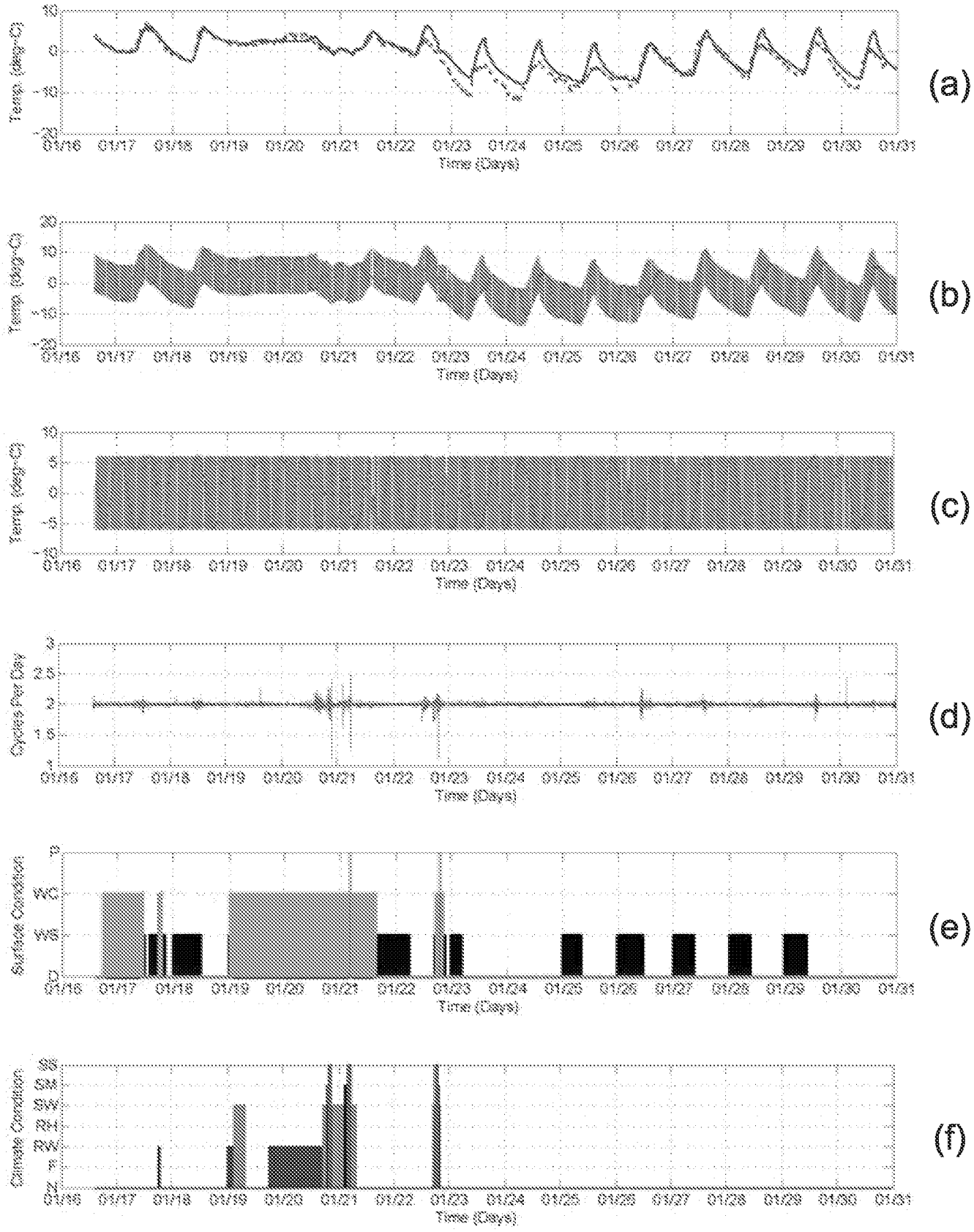
Temp. (deg-C)
Time (Days)
(a)
Temp (top)-C)
Time (Days)
(b)
Temp. (deg-C)
Time (Days)
(c)
Cycles Per Day
Time (Days)
(d)
Surface Condition
P
WC
WS
D
Time (Days)
(e)
Climate Condition
SS
SM
SW
RH
RW
F
N
Time (Days)
(f)
01/16 01/17 01/18 01/19 01/20 01/21 01/22 01/23 01/24 01/25 01/26 01/27 01/28 01/29 01/30 01/31

FIG. 13

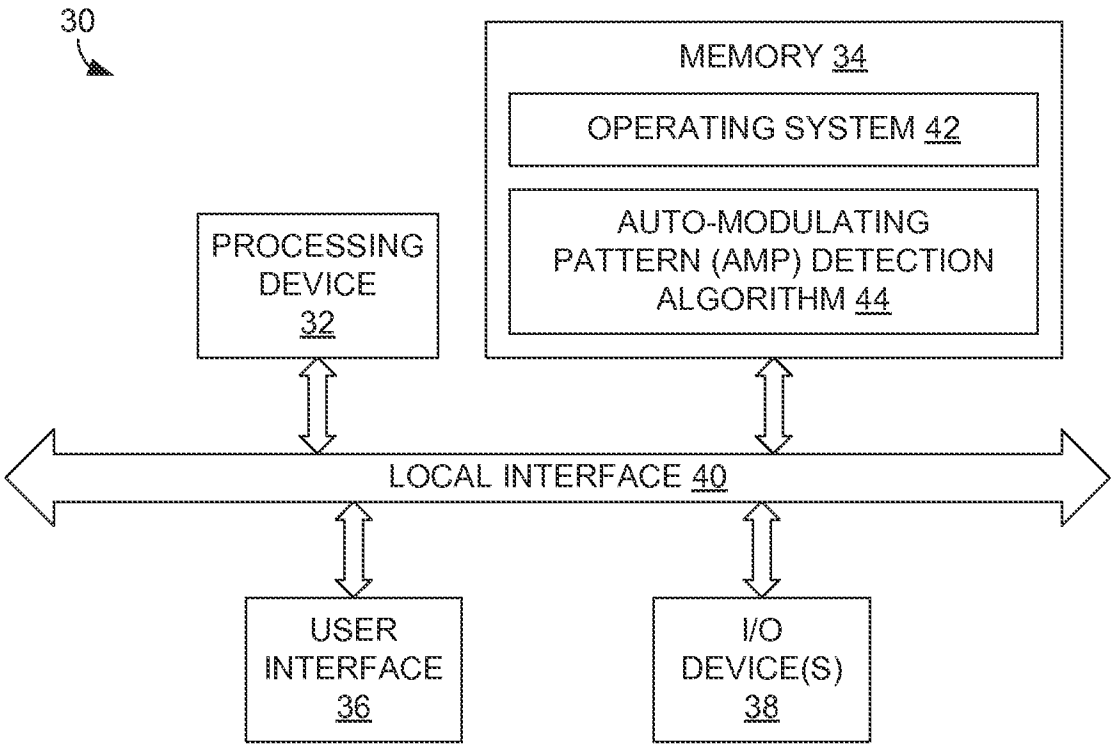
30
MEMORY 34
OPERATING SYSTEM 42
AUTO-MODULATING PATTERN (AMP) DETECTION ALGORITHM 44
PROCESSING DEVICE 32
LOCAL INTERFACE 40
USER INTERFACE 36
I/O DEVICE(S) 38

FIG. 14